

## Intermediate frequency modes in Raman spectra of Ar<sup>+</sup>-irradiated single-wall carbon nanotubes

Viera Skákalová<sup>1</sup>, Janina Maultzsch<sup>2</sup>, Zoltán Osváth<sup>3</sup>, László P. Biró<sup>3</sup>, and Siegmar Roth<sup>1</sup>

<sup>1</sup> Max Planck Institute for Solid State Research, Heisenbergstraße 1, 70569 Stuttgart, Germany

<sup>2</sup> Institut für Festkörperphysik, Technische Universität Berlin, Hardenbergstraße 36, 10623 Berlin, Germany

<sup>3</sup> Research Institute for Technical Physics and Material Science, Hungarian Academy of Sciences MFA, 1525 Budapest, Hungary

Received 2 April 2007, revised 25 April 2007, accepted 26 April 2007

Published online 4 May 2007

PACS 61.80.Jh, 78.30.Na, 78.67.Ch

We study the effect of Ar<sup>+</sup> irradiation on the intermediate frequency modes (IFM) in Raman spectra of single-wall carbon nanotubes. We observe new features in the intermediate frequency region from 386 to 635 cm<sup>-1</sup> as the defect concentration increases, whereas at the same time there is a decrease of

other IFM modes. After annealing in vacuum, the IFM modes recover and become similar to those of the nanotubes before irradiation. We interpret the new features in the Raman spectra as originating from the phonon density of states that becomes visible in the Raman process due to the presence of defects.

phys. stat. sol. (RRL) 1, No. 4, 138–140 (2007) / DOI 10.1002/pssr.200701069

# Intermediate frequency modes in Raman spectra of Ar<sup>+</sup>-irradiated single-wall carbon nanotubes

Viera Skákalová<sup>\*1</sup>, Janina Maultzsch<sup>\*\*2</sup>, Zoltán Osváth<sup>3</sup>, László P. Biró<sup>3</sup>, and Siegmur Roth<sup>1</sup>

<sup>1</sup> Max Planck Institute for Solid State Research, Heisenbergstraße 1, 70569 Stuttgart, Germany

<sup>2</sup> Institut für Festkörperphysik, Technische Universität Berlin, Hardenbergstraße 36, 10623 Berlin, Germany

<sup>3</sup> Research Institute for Technical Physics and Material Science, Hungarian Academy of Sciences MFA, 1525 Budapest, Hungary

Received 2 April 2007, revised 25 April 2007, accepted 26 April 2007

Published online 4 May 2007

PACS 61.80.Jh, 78.30.Na, 78.67.Ch

\* Corresponding author: e-mail v.skakalova@fkf.mpg.de, Phone: +49 711 689 1434, Fax: +49 711 689 1010

\*\* Present address: Departments of Physics and Electrical Engineering, Columbia University, New York, NY 10027, USA

We study the effect of Ar<sup>+</sup> irradiation on the intermediate frequency modes (IFM) in Raman spectra of single-wall carbon nanotubes. We observe new features in the intermediate frequency region from 386 to 635 cm<sup>-1</sup> as the defect concentration increases, whereas at the same time there is a decrease of

other IFM modes. After annealing in vacuum, the IFM modes recover and become similar to those of the nanotubes before irradiation. We interpret the new features in the Raman spectra as originating from the phonon density of states that becomes visible in the Raman process due to the presence of defects.

© 2007 WILEY-VCH Verlag GmbH & Co. KGaA, Weinheim

**1 Introduction** Raman spectroscopy is one of the most powerful tools for characterizing carbon nanotubes [1]. Four main features dominate the Raman spectra of single-wall carbon nanotubes (SWNT): (i) the RBM (radial breathing mode, 100 to 400 cm<sup>-1</sup>), which characterizes the tube diameter; (ii) the *D*-mode (1300 to 1360 cm<sup>-1</sup>), which is induced by structural defects [2]; (iii) the *G*-mode (1500–1600 cm<sup>-1</sup>), which can give information about the presence of metallic tubes in the SWNT sample; and (iv) the *D*\*-mode (about 2600 cm<sup>-1</sup>), the second-order overtone of the *D*-mode. Besides these modes, attention has recently turned towards weak Raman features in the intermediate frequency region (IFM) between 600 and 1100 cm<sup>-1</sup>. Some of the IFM modes appear only over a certain range of excitation energies, resulting in a step-like dispersion of the peaks with the energy of the incident photons. Others (at 700, 850, 1050 cm<sup>-1</sup>) remain visible at all excitation wavelengths [3–5]. In Refs. [3, 4], this phenomenon is explained by a combination of optical and acoustic phonon modes.

In this letter we discuss additional features in the intermediate frequency region of the Raman spectra of SWNTs which appear after ion- or  $\gamma$ -irradiation [6–8]. Introducing defects into the nanotube structure allows us to directly distinguish between defect-induced peaks in the

IFM region and those that are always Raman-allowed. As the defect concentration increases, the intensities of the IFM modes at higher frequencies decrease, while the newly observed features at about 420 and 620 cm<sup>-1</sup> show an increase in intensity. We interpret these new features as originating from the phonon density of states that becomes visible in the Raman process due to the presence of defects. In addition, we observe Raman peaks corresponding to the second-order modes of the RBM.

**2 Experimental details** Purified HiPCO SWNTs were purchased from Carbon Nanotechnologies, Inc. (Texas). The SWNT film was introduced into an ion implanter and irradiated with Ar<sup>+</sup> ions of 30 keV, using doses from  $5 \times 10^{11}$  ions/cm<sup>2</sup> up to  $4 \times 10^{12}$  ions/cm<sup>2</sup>. The ion current density was  $I = 0.9$  nA/cm<sup>2</sup> at normal incidence [9].

Raman spectra were measured using microscope Raman spectroscopy with a Jobin Yvon–LabRam spectrometer. The laser excitation wavelength was 633 nm; the spectral resolution was 4 cm<sup>-1</sup>.

**3 Results and discussion** Figure 1 shows Raman spectra of pristine and Ar<sup>+</sup>-irradiated SWNT samples. The *D*-mode at 1302 cm<sup>-1</sup> is a result of double-resonant scatter-

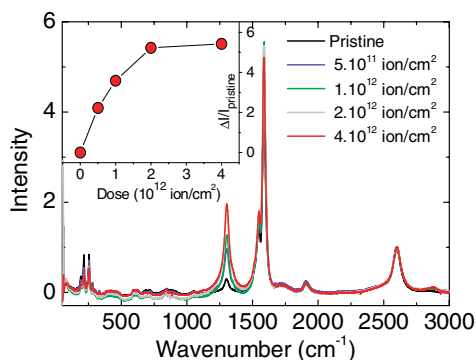


**Figure 1** (online colour at: www.pss-rapid.com) Raman spectra of pristine and  $\text{Ar}^+$  irradiated (up to  $4 \times 10^{12}$  ions/ $\text{cm}^2$ ) SWNTs. Inset: Relative intensity change  $\Delta I/I_{\text{pristine}}$  of the Raman  $D$ -mode vs. dose of  $\text{Ar}^+$  ions.

ing induced by structural defects in the nanotube [10, 11]; in our case, its intensity increase reflects the damage caused by  $\text{Ar}^+$  irradiation.

The second-order overtone,  $D^*$ , does not require defects. Its intensity does not scale with defect concentration. Therefore we normalize all the presented Raman spectra to that of the defect-independent  $D^*$ -mode intensity. In order to evaluate the effect of  $\text{Ar}^+$  irradiation on different modes of the spectra, we compare for each mode in the IFM region the relative intensity changes  $\Delta I/I_{\text{pristine}}$  (where  $\Delta I = I_{\text{irradiated}} - I_{\text{pristine}}$ ). The dependence of the relative intensity change of the  $D$ -mode is plotted in inset of Fig. 1: with rising dose, we observe a steep growth of the relative intensity change, saturating close to 550%. In our previous work [8], we interpreted a similar effect due to  $\gamma$ -irradiation as the result of equilibrium in the dynamics of creation and recombination of the defects. To quantify the structural damage caused by ion irradiation at a dose of  $10^{12}$  ions/ $\text{cm}^2$ , we evaluate that a SWNT of 1 nm in diameter and 1  $\mu\text{m}$  in length would be hit 10 times on average, creating approximately 10 to 20 defects in the wall of the SWNT.

In Fig. 2 we show the intermediate frequency region for the pristine sample and for the sample irradiated with a dose  $4 \times 10^{12}$  ions/ $\text{cm}^2$  of  $\text{Ar}^+$  ions. We observe several broad bands at  $386\text{--}490\text{ cm}^{-1}$ ,  $585\text{--}635\text{ cm}^{-1}$ ,  $670\text{--}730\text{ cm}^{-1}$ ,  $1000\text{--}1100\text{ cm}^{-1}$ , and a relatively sharp peak at  $845\text{ cm}^{-1}$  with a shoulder extended up to  $980\text{ cm}^{-1}$ . In Fig. 3, the relative intensity change  $\Delta I/I_{\text{pristine}}$  of these modes is plotted as a function of the irradiation dose. We observe two different types of behavior: some of the modes increase in intensity with larger defect concentration, whereas others become weaker. The relative changes of intensity for the two lower-frequency bands at  $386\text{--}490\text{ cm}^{-1}$  and  $585\text{--}635\text{ cm}^{-1}$  (Fig. 3) grow with increasing defect concentration up to 500%, similarly to the  $D$ -mode (Fig. 1). In contrast, the bands around  $670\text{--}730\text{ cm}^{-1}$ ,  $1000\text{--}1100\text{ cm}^{-1}$  and the shoulder at  $775\text{--}980\text{ cm}^{-1}$  slightly decrease. The sharp peak at  $845\text{ cm}^{-1}$  shows a weak increase with increasing irradiation dose. It indicates that the nature of the peak at  $845\text{ cm}^{-1}$  might be different from the other non-dispersive features ( $720, 1050\text{ cm}^{-1}$ ) in Refs. [3, 4].

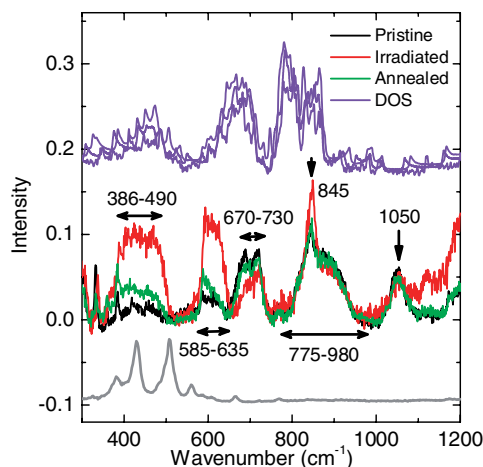


**Figure 2** (online colour at: www.pss-rapid.com) IFM region of Raman spectra of pristine SWNTs (black line) compared to  $\text{Ar}^+$  irradiated ( $4 \times 10^{12}$  ions/ $\text{cm}^2$ ) SWNTs (red line) and after (green) annealing in vacuum at  $960\text{ }^\circ\text{C}$  measured with excitation wavelength  $633\text{ nm}$ . Gray line: RBM region of the pristine sample vs. doubled wavenumber scale. The plots in blue are calculations of the phonon DOS for SWNT with various diameters.

The  $\text{Ar}^+$  irradiated SWNT film with the dose  $4 \times 10^{12}$  ions/ $\text{cm}^2$  was then annealed in vacuum at  $960\text{ }^\circ\text{C}$  for four hours. The overall recovery of the defective SWNT structure after annealing is clearly demonstrated in Fig. 2 (green line). All the IFM features of the irradiated sample change substantially after annealing and become similar to the original features of the pristine sample.

When defects are introduced into the sample, the translational symmetry is disturbed and hence the momentum conservation requirement in the Raman process is relaxed. Therefore, phonons with wave vectors from throughout the Brillouin zone can contribute to the spectrum. In case of non-resonant scattering, the spectrum then resembles the phonon density of states, besides the resonantly enhanced modes like  $D$  and  $D^*$ . As the two lower-frequency bands in Fig. 2 increase with defect concentration, we assign them to contributions from the phonon density of states. The higher-frequency peaks, which are also broad and apparently do not come from a single phonon mode, are probably due to two-phonon scattering, not requiring defects. A

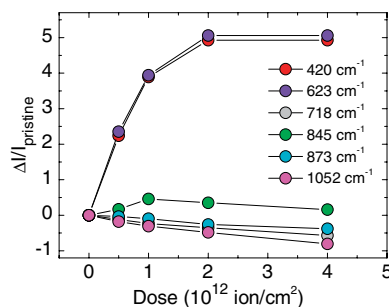


**Figure 3** (online colour at: www.pss-rapid.com) Relative intensity change  $\Delta I/I_{\text{pristine}}$  of the IFM modes vs. dose of  $\text{Ar}^+$  ions.

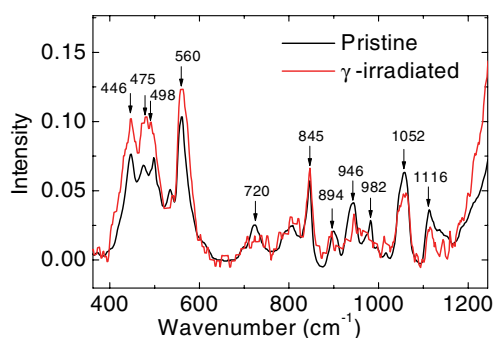


**Figure 4** (online colour at: [www.pss-rapid.com](http://www.pss-rapid.com)) IFM of pristine and  $\gamma$ -irradiated SWNT at excitation wavelength 1054 nm.

two-phonon process probes phonons from the entire Brillouin zone, because only the sum of the two phonon wavevectors must be approximately zero. Therefore, the two-phonon modes can be observed even if no defects are present. They decrease with increasing defect concentration, as the crystal structure is damaged. In nanocrystalline graphite similar features were observed around 450  $\text{cm}^{-1}$  and 800  $\text{cm}^{-1}$  [12] and attributed to the phonon DOS.

To further assign the observed modes, we compare in Fig. 2 the measured IFMs with a force-constants calculation of the phonon density of states (blue lines) [13, 14]. The phonon density of states was numerically calculated from the phonon dispersion in Ref. [13] by summing over all bands and phonon wave vectors per energy interval. The experimental lineshape indeed resembles the phonon density of states. Both lower-frequency bands can be tentatively assigned to modes that are derived from the two lowest  $M$ -point phonons in graphene. The band centered at 440  $\text{cm}^{-1}$  might in addition contain contributions from RBM-like modes with band index  $m \neq 0$  (degenerate modes). We attribute the broad band (775–980  $\text{cm}^{-1}$ ) to overtones of the phonons in the bands at 386–490  $\text{cm}^{-1}$ ; this is consistent with the observation that it does not increase with defect concentration. We assume that the overtones of the second newly observed band at 585–635  $\text{cm}^{-1}$  are hidden in the left shoulder of the  $D$ -mode.

In addition, the IFM region of the pristine sample contains several sharp peaks at twice the frequency of some RBMs, see e.g. the peak at 385  $\text{cm}^{-1}$ . These are second-order overtones of the RBM; they decrease with defect concentration. For visualization, we plot the RBMs of the pristine sample against a doubled wavenumber scale (gray line, bottom of Fig. 2). Whether particular RBM peaks have a strong second-order overtone depends on the electron-phonon coupling for the given nanotube [15]; the resonance profiles and RBM intensities will be analyzed elsewhere.

To demonstrate a general aspect of the observed phenomena, we present results in Fig. 4 showing the same effect on the IFM modes due to defects introduced by  $\gamma$ -irradiation. The data were presented in our previous work [8]; however, the IFM region was not analyzed in detail. A clear effect of structural damage after  $\gamma$ -irradiation can be observed also in the IFM region, although less pronounced

than after ion-irradiation. After  $\gamma$ -irradiation, the intensities of the first group of peaks from 446 to 560  $\text{cm}^{-1}$  increase, while the intensities of the peaks at twice the frequency (from 894 to 1116  $\text{cm}^{-1}$ ) decrease. As for the Ar<sup>+</sup>-irradiated samples, the three higher-frequency, “non-dispersive” modes [3–5] do not behave the same way: while the modes at  $\sim 720$  and 1050  $\text{cm}^{-1}$  decrease after exposing the SWNT sample to  $\gamma$ -rays, the one at 845  $\text{cm}^{-1}$  increases, contrary to the previous ones. This is again an indication that the mode at 845  $\text{cm}^{-1}$  is of a different origin. The positions of the bands observed with 1054 nm wavelength compared to those excited at 633 nm, are shifted towards higher frequencies. The dispersion of IFMs with excitation wavelength might reflect a dependence of the phonon DOS on nanotube diameter.

**4 Conclusion** We have shown that ion irradiation causes significant damage to the SWNT structure, as demonstrated by a manifold increase of the  $D$ -mode intensity. We observe new modes in the IFM region at about 420 and 620  $\text{cm}^{-1}$ , which grow as the defect concentration increases, whereas higher-frequency IFM modes decrease. We interpret the new IFM features in the Raman spectra as originating from the phonon density of states that becomes visible due to the presence of defects. The higher-frequency modes, in contrast, are assigned to overtones of the defect-induced peaks. The different behaviour of the IFM modes with changing defect concentration supports our assignment.

**Acknowledgements** This work was supported by EC projects SPANG and SANES. Z.O. and L.P.B. thank for financial support from OTKA grant T043685, NKTH and MOFENACS. J.M. acknowledges support from the Alexander-von-Humboldt foundation. We thank Martin Hulman for the Raman measurement with excitation wavelength 1054 nm.

## References

- [1] S. Reich, C. Thomsen, and J. Maultzsch, *Carbon Nanotubes: Basic Concepts and Physical Properties* (Wiley-VCH, Weinheim, 2004).
- [2] F. Tuinstra and J. L. Koenig, *J. Chem. Phys.* **53**, 1126 (1970).
- [3] C. Fantini et al., *Phys. Rev. Lett.* **93**, 087401 (2004).
- [4] C. Fantini et al., *Phys. Rev. B* **72**, 085446 (2005).
- [5] M. Kalbac, L. Kavan, M. Zúkalová, and L. Dunsch, *Chemistry* **12**, 4451 (2006).
- [6] V. Skákalová, M. Hulman, P. Fedorko, P. Lukáč, and S. Roth, *AIP Conf. Proc.* **685**, 143 (2003).
- [7] V. Skákalová et al., *Diamond Relat. Mater.* **13**, 296 (2004).
- [8] M. Hulman, V. Skákalová, S. Roth, and H. Kuzmany, *J. Appl. Phys.* **98**, 024311 (2005).
- [9] Z. Osváth, G. Vértesy, L. Tapasztó, F. Wéber, Z. E. Horváth, J. Gyulai, and L. P. Biró, *AIP Conf. Proc.* **786**, 154 (2004).
- [10] C. Thomsen and S. Reich, *Phys. Rev. Lett.* **85**, 5214 (2000).
- [11] J. Maultzsch, S. Reich, and C. Thomsen, *Phys. Rev. B* **64**, 121407(R) (2001).
- [12] F. Li and J. S. Lannin, *Appl. Phys. Lett.* **61**, 2116 (1992).
- [13] J. Maultzsch, S. Reich, C. Thomsen, E. Dobardžić, I. Milošević, and M. Damnjanović, *Solid State Commun.* **121**, 471 (2002).
- [14] E. Dobardžić et al., *Phys. Rev. B* **68**, 045408 (2003).
- [15] Y. Yin et al., *Phys. Rev. Lett.* **98**, 037404 (2007).